Available online at www.sciencedirect.com

ScienceDirect

Transportation Research Procedia 70 (2023) 218–225

Transportation Research Procedia

www.elsevier.com/locate/procedia

8th International Electric Vehicle Conference (EVC 2023)

Impact of multiple ultrasonic and laser welds on electro-thermal behaviours for connecting Li-ion battery cells

Indranil Manna[a], Nikhil Kumar[b], Abhishek Das[a,b,*]

[a]*Department of Mechanical Engineering, Indian Institute of Technology Delhi, New Delhi, 110016, India*
[b]*WMG, The University of Warwick, Coventry CV4 8GJ, United Kingdom*

Abstract

The need for efficient manufacturing methods to produce battery packs is increasing with the growing demand for Electric Vehicles (EVs). A large number of individual battery cells are interconnected to meet the power and capacity requirements of EVs. As a result, several joining methods are under investigation to produce battery interconnects efficiently. Typically, ultrasonic metal welding is employed to produce pouch cell tab-to-tab interconnects. In addition, laser welding is also emerging as a fast and non-contact joining alternative. Detailed critical-to-quality investigations are needed to compare both joint types. This paper investigated the effect of multiple ultrasonic nuggets and laser seams on electrical resistance and thermal performance at the tab-to-tab interconnects. Multi-physics simulation models were developed to predict the joint resistance and temperature rise under different charge-discharge current values. Results show that electrical contact resistance was decreased by 54% when a 5 mm diameter circular laser weld-based tab-to-tab connection was replaced with six circular welds of the same diameter. Simulation-based comparative analysis showed that resistance and temperature rise obtained from the 3 or 6 circular laser welds were similar to 3 or 6 nuggets ultrasonic welds. As a result, both the ultrasonic and laser joints can be used as per need.

Keywords: Electric vehicles; laser welding; ultrasonic metal welding; joint resistance; temperature rise

1. Introduction

There is an emerging interest in electric cars (EVs) to reduce carbon emissions from the transportation industry due to rising environmental concerns. Traditional automobiles powered by fossil fuels significantly contribute to air pollution and climate change, and the shift to EVs provides an opportunity to address these issues. As part of its commitment to the Paris Agreement on climate change, India plans to achieve 30% electric mobility by 2030, as

* Corresponding author. Tel.: +91 (0)11 2654 8581.
E-mail address: abhi@mech.iitd.ac.in

2352-1465
10.1016/j.trpro.2023.11.022

decided by NITI Aayog (2021). In addition, several national and international legislations are driving the adaptation of EVs, and the demand for electric vehicles is increasing. Therefore, the demand for efficient manufacturing of battery packs to be used in EVs is also growing.

1.1. Market Demand

Electric Vehicles are powered by a battery pack assembled by several battery modules. Modules are structured by assembling multiple numbers of individual battery cells. Efficient manufacturing of electric vehicles (EVs) battery packs is in high demand to meet the high-volume production need. To connect the individual cells into modules, efficient joining methods are needed. Ultrasonic metal welding and laser welding are the most suitable joining methods to produce tab-to-tab or tab-to-busbar connections for pouch cells, as identified by (Das et al., 2018). These joints must satisfy the critical-to-quality criteria, such as low electrical resistance and temperature rise at the joint during charge-discharge conditions. Therefore, effective battery interconnects joining technologies are needed to satisfy the industrial demand and critical-to-quality criteria.

1.2. Research Gaps and Objectives

Both laser and ultrasonic welding is suitable for producing tab-to-tab dissimilar thin metal welding, where ultrasonic metal welding is a solid-state welding and laser is a fusion-based joining process. Due to ohmic heating at the weld joint, temperature rise should be minimum such that the battery operation is safe and does not degrade the temperature-sensitive electrolyte inside the battery cell. To investigate the joint resistance and temperature rise, a few investigations were performed by researchers. Dimatteo et al. (2019) investigated Al and Cu thin sheets for laser micro-welding and reported that the joint resistance resulted from the intermetallic compound formation and brittle joint. Kah et al. (2015) studied the various possible intermetallic compounds formation for Al and Cu in different welding processes. Mehlmann et al. (2014) performed a wobbling laser beam to join CuSn6 copper tabs with a cylindrical cell and measured the connection resistance using a four-wire technique. A linear stitch of 5 mm laser joint exhibited resistance ranging from 0.3 to 0.5 mΩ. In a separate study, Brand et al. (2015) measured the electrical contact resistance between the cylindrical cell terminal and CuZn37 tabs welded by laser welding. The investigation determined a minimum electrical contact resistance of 0.13 mΩ. Mohd Isa et al. (2023) investigated friction stir welding, where it was found that graphene inside the copper-aluminium joint, reduces the electrical resistance. Ni et al. (2022) studied the effect of Cu nanoparticles inside Cu/Cu ultrasonic welding, where a 5.9% electrical resistance reduction was noted. Shaikh et al. (2019) also found the effect of laser processing parameters on joint strength, microstructure, joint resistance, and temperature rise. Kumar et al. (2021) have also evaluated the intermetallic compound and resistance due to laser welding with numerous material combinations.

In the literature, research was mainly focused on electrical and thermal characterisation considering single-joint configuration, as reported by Solchenbach et al. (2014). Wang et al. (2015) developed a thermal model to predict the possible causes of thermal runaway risks of the battery. Sadeghian et al. (2022) investigated the blue laser application for joining Cu and mild steel and found better weld strength. In addition, Das et al. (2022) have studied the effect of different seam sizes of laser micro joints on the resistance of the weld joint and its temperature rise. Furthermore, Kumar et al. (2022) investigated four nugget resistance spot welded joints resistance and temperature behaviours using nickel-to-steel stack-ups and thereafter, applied a novel micro-resistance welding technique to reduce cycle time and its utilisation for EV battery manufacturing (Kumar et al., 2023). However, the impact of placing multiple ultrasonic weld nuggets or laser welded seams on electrical resistance and temperature rise at the tab-to-tab interconnects has yet to be fully understood when charge/discharge current is applied. There are limited studies on the effect of placing multi-joints by LBW and USW on the electric resistance and its corresponding temperature rise. Therefore, this paper focused on identifying the effect of joint electrical resistance and thermal performances using an electro-thermal multi-physics model where multiple laser seams and ultrasonic weld nuggets were compared with experimental verification and validation.

2. Methodology

2.1. Experimental Investigation

2.1.1. Material and Joint Configuration

Typically, nickel-plated copper (Cu[Ni]) and aluminium (Al) are used as tab terminal materials in the pouch cell. Therefore, Cu[Ni] tabs of 45×45×0.3 mm and Al tabs of 45×45×0.4 mm have been selected for this study. Al was welded on top of Cu[Ni] in Lap joint configuration with an overlap zone of 25×45 mm. A schematic diagram of the joint configuration is shown in Fig.1(a). Multi-weld joints were by laser welding and ultrasonic metal welding. Test samples were prepared considering 1, 3, and 6 laser seams or ultrasonic nuggets, as shown in Fig.1(b). The laser seams were 5 mm in diameter and ultrasonic nuggets were of rectangular shape of 5×10 mm.

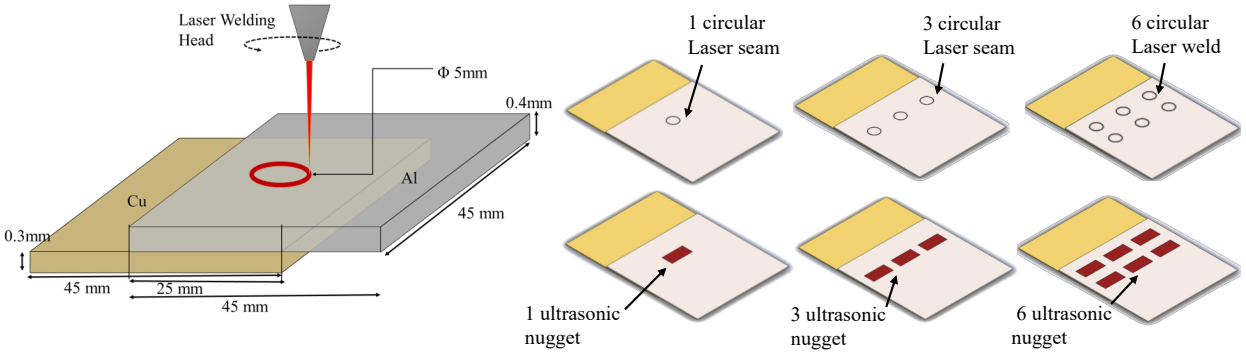

Fig. 1. (a) Schematic of (a) joint configuration using laser welding, (b) test samples of 1, 3, and 6 laser seams and ultrasonic nuggets

2.1.2. Laser Welding Parameter

A YLR-150W Quasi-CW IR laser having 1.5 kW peak power supplied by IPG Photonics was used for producing the laser seams in this study. From initial screening studies, the laser welding parameters were finalised. The laser power was set at 450 W (i.e., 30% of the peak power) and the spot diameter was 28 µm. Although the IR laser has a high reflectivity with Cu and Aluminium, due to having a single-mode laser, melting of the metal can be performed with less laser power. The laser pulse frequency was set to 50 Hz, and the laser pulse-on time was 2 msec with a welding speed of 500 mm/min. The laser wobble head, FLW-D30, was used with the air-cooled wobble functionality in a vertical configuration (Kumar et al., 2021). Circular laser wobbling with an amplitude of 0.4 mm and wobble frequency of 600 Hz was performed to get the circular seam of the weld zone. Argon was used as a shielding gas at the flow rate of 20 L/min. For laser welding, tab-to-tab connections were produced with 1, 3 and 6 circular seams with a diameter of 5 mm each, as shown in Fig. 1(b).

2.1.3. Ultrasonic Welding Parameter

The ultrasonic metal welding was performed using a Telsonic MPX ultrasonic welding system with a clamping force range of up to 5 kN and a peak power of 6.5 kW. The anvil of the welding setup was made of steel, while the horn contained a mixture of titanium alloy. The welds were achieved by clamping the sheets in between the horn and the anvil. In this study, ultrasonic frequency 20 kHz, welding pressure 2.5 bar, amplitude 50 µm, and welding time 0.3 sec were used to produce ultrasonic weld nuggets (Singh et al., 2022). The tab-to-tab connections were produced with 1, 3, and 6 ultrasonic nuggets as shown in Fig. 1(b).

2.1.4. Setup for Electrical and thermal characterization

After conducting the laser micro-welding and the ultrasonic metal welding, the electrical resistance of the weld joint and its correspondence thermal rise of the samples were tested. Due to joule heating or ohmic heating, the heat

was generated at the joint due to the application of electrical current flow through the joint. Bandhauer et al. (2011) explained, for the safety issue of the battery, while charging and discharging, the joint temperature rise due to this heating should be inside a specific constraint. For measuring the joint resistance, the current from the constant current supply was passed through the points on both sheets (Fig. 2) and the voltage drop in between the points was measured by the point probe-based voltage sensors. A 50-amp current was supplied for 3 min to measure the joint resistance for each coupon sample to avoid heat generation at the joint. For measuring the temperature rise, a thermal camera was placed on the top of the weld zone. As temperature rise also depends on the amplitude of the currents, 100-, 150- and 200-amp currents were passed for 3 min in this study. The temperature rise of each sample was recorded from room temperature (~23°C), and then compared over different weld seam/nugget numbers for a specific current amplitude.

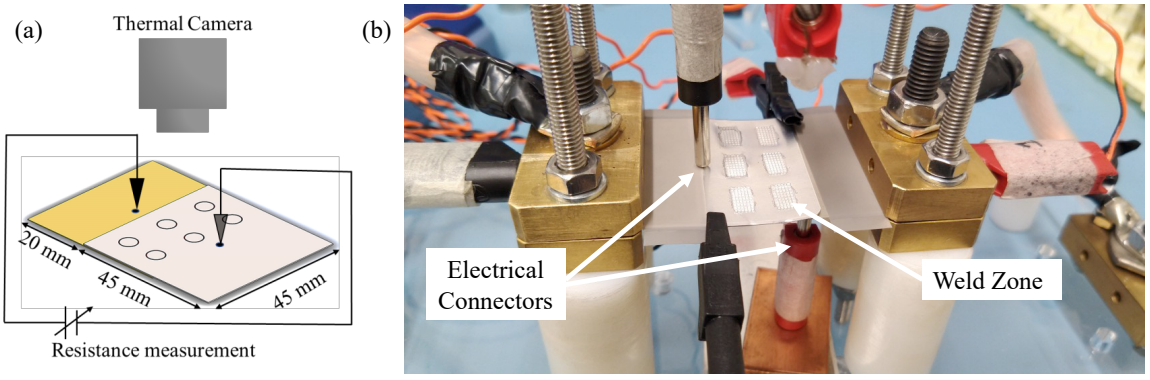

Fig. 2. Joint resistance and temperature measurement (a) schematic representation with voltage drop measurement points (showing 6 laser seams), and (b) experimental test setup for measurement (showing 6 ultrasonic nuggets).

2.2. Electrical and Thermal Model Development

Numerical models of the laser and ultrasonic joints were developed by using COMSOL Multi-physics, where Cu[Ni] and Al were used as tab materials (Fig. 1). The initial temperature was also set at 23°C due to ambient temperature conditions. Using element size settings such as maximum element size = 1.0 mm, minimum element size = 0.3 mm, element growth rate = 1.5, and curvature factor = 0.4, the structured tetrahedral mesh was produced. To identify the change in resistance and temperature, a specific relationship between temperature-dependent conductivity with applied current and a linearized resistivity model was used (Sibilia et al., 2021). A similar temperature-dependent resistivity model, developed by Das et al. (2022), was used in this study to simulate the effect of joint resistance and temperature rise when multiple weld seams from laser welding and weld nuggets from ultrasonic metal welding are subjected to use. Convective heat transfer, which is the leading method of heat dissipation in this case, can be described by the convective heat flux, which was applied to the surfaces of the specimen, as $q=h\times(T_{ext}-T)$, where h is the heat transfer coefficient and T_{ext} is the external ambient temperature. For model development, the h value was taken as 9.5 W/m^2K, which was selected based on the training model data. Models have been simulated for three different applied currents 100-, 150-, and 200-amp with input current densities of 7.4×106, 11.1×106, and 14.8×106 amp/m^2, respectively. The model has been trained on 150-amp applied current and validated with 100 and 200-amp current values. The material properties used for developing the electro-thermal model are listed in Table 1.

Table 1. Material properties used in the model development.

Properties	Material		
	Cu[Ni] (C101S)	Al	Weld seam/nugget
Density, ρ [kg/m^3]	8960	2700	5200
Thermal Conductivity, k [W/(m·K)]	400	238	110
Heat capacity, C_p [J/(kg·K)]	385	900	385
Reference resistivity, ρ_0 [Ω·m]	1.72e-08	2.64e-08	6.5e-8
Resistivity temperature coefficient, α [1/K]	0.003	0.00429	0.0043

3. Results and Discussion

3.1. Analysis of joint resistance

It was observed that a single circular laser seam had a maximum joint resistance of 0.054 mΩ from the experimental data, which was decreased by 37.04%, and 53.70% for 3 and 6 seams [Fig. 3(a)]. Similarly for ultrasonic welding, the highest resistance was noticed in the single nugget specimen, which was about 0.043 mΩ. By increasing the weld nuggets to 3 and 6, the joint resistance was decreased by 18.60% and 27.90%, respectively.

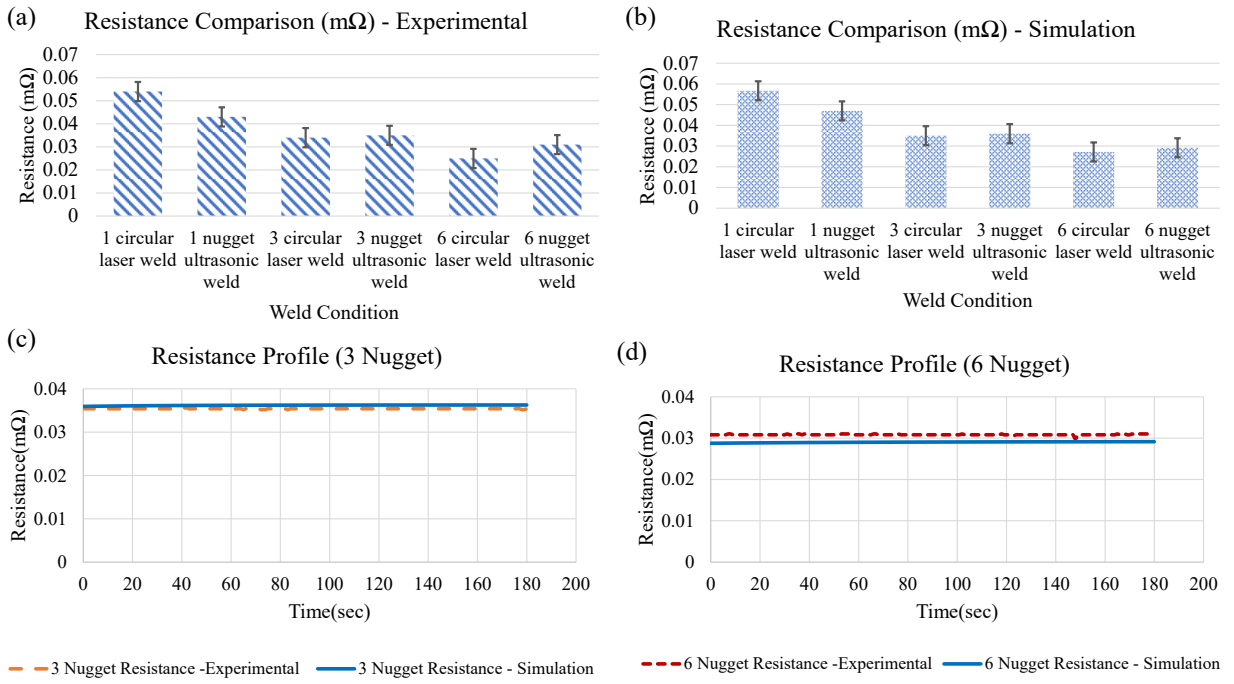

Fig. 3. Resistance comparison data in various weld seams or nuggets (a)Experimental results, (b) Simulation results, and (c) - (d)Verification of the simulated data with the experimental data using 3 and 6 nuggets ultrasonic joints.

In general, the resistance value decreased with the increasing number of weld nuggets/seams. Fig. 3 also reports the comparison between the laser and ultrasonic welding joint resistance. The simulation-based resistance data for laser seams and ultrasonic nuggets are shown in Fig. 3(b). The resistance value for 1 circular laser weld is higher than the 1 nugget ultrasonic welding. But by increasing the number of weld seams, the laser welded samples' joint resistance was lower than ultrasonic weld nuggets. In Fig. 3(c, d), the simulation model-generated resistance values obtained from the 3 and 6 ultrasonic weld nuggets were validated with the experimental data. For passing 50 amp current for 3 min, simulation-generated resistance profiles have been found to be similar to the experimental resistance with a maximum error of 2.42% for 3 nuggets and 5.35% for 6 nuggets ultrasonic welded samples. Therefore, the simulation model can be used at the early design stage to predict the joint resistance, and battery manufacturing engineers can use this model to minimise overall battery module or pack resistance.

3.2. Predicting temperature profile with verification and validation

The developed model has been validated with the joint resistance and the temperature rise for continuous current flow conditions. The temperature profiles obtained by applying 150 amp current for 3 mins are shown in Fig. 4(a) where the simulation predicted temperature profiles for the 1 and 3 circular laser welds were compared with the

experimental test data. The convective heat transfer value has been taken as 9.5 W/m2K, which highly depended on the intermetallic compound formation between Cu and Al in the weld zone (Das et al., 2022). The results showed that the simulation-predicted profiles closely followed the temperature profile obtained from the experimental results with a maximum error of 4%. Thereafter, the simulation model was used to predict the temperature profiles for different current values as well as other weld seams. For 100-amp current flow, the 3 and 6 circular laser welded seams were tested for temperature rise and validated with experimental data. The maximum temperatures obtained from the simulation and experimental test were 34.82°C and 34.4°C, respectively when 3 circular laser weld sample was used for 100-amp current flow conditions, see Fig. 4(c). Similarly, in the case of 6 circular laser weld samples, the maximum temperature obtained from the experiment was 31.48°C and the simulation predicted value was 33.8°C when 100-amp current flow condition was used, as reported in Fig. 4(b). For 200-amp current passing through the 3 circular laser weld samples, temperature profiles are shown in Fig. 4(d), which is also similar to the actual temperature rise profile.

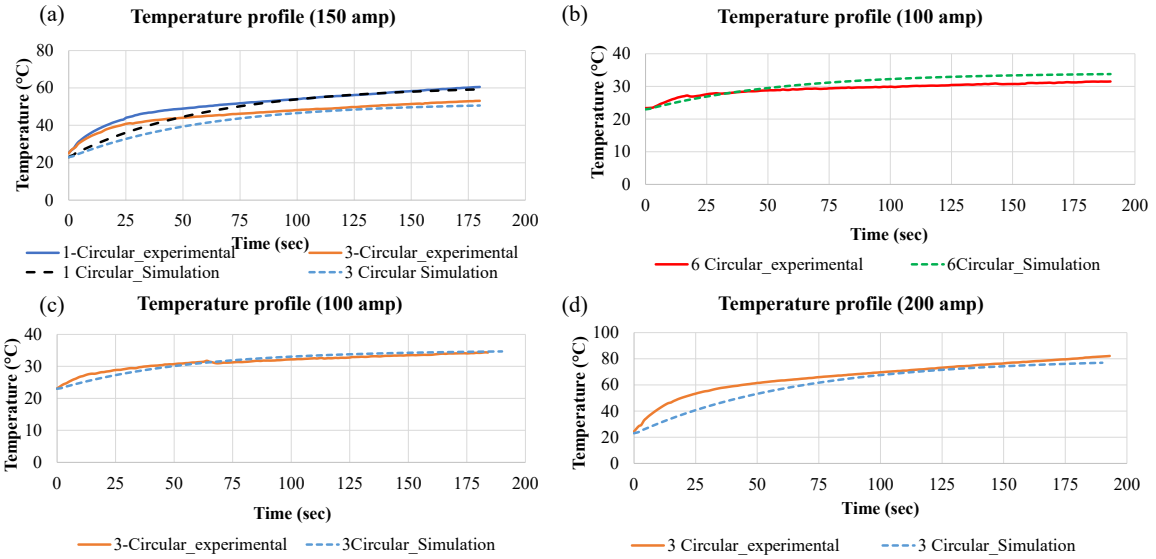

Fig. 4. Temperature rise profiles (a) simulation data validation with the experimental data using 150 amp current for 1 and 3 circular laser weld samples, and validation of simulation model with different parameters (b) 100 Amp-6 circular laser weld, (c) 100 Amp-3 circular laser weld, (d) 200 Amp-3 circular laser weld conditions.

3.3. Simulation-based analysis of the temperature rise

The temperature rise at the weld joint due to the ohmic heating was proportional to the joint resistance, as shown in Fig. 5. The simulation-based joint temperature response profiles for different weld conditions have been plotted for 100-amp, 150-amp, and 200-amp current applications for 3 min at the weld joint, refer to Fig. (a) – (c). For all the welding conditions, 1 circular shows the maximum temperature rise. This simulation-based temperature profile will be helpful in understanding the critical condition of the battery design. In the case of 6 circular laser seam-based samples, the maximum temperatures were about 33.88°C, 48.8°C, and 72.7°C for 100-amp, 150-amp, and 200-amp current supply for 3 min, respectively. Again, in the case of 6-nugget ultrasonic welding, these values are 33.86°C, 48.74°C, and 72.39°C, respectively. Fig. 5(d) shows a comparison of maximum joint temperature rise between laser welding and ultrasonic welding for 150-amp current flow. Fig. 5(e) shows the simulated temperature responses obtained when 1, 3 and 6 circular laser seams and ultrasonic nuggets were subjected to 150-amp current flow for 3 min.

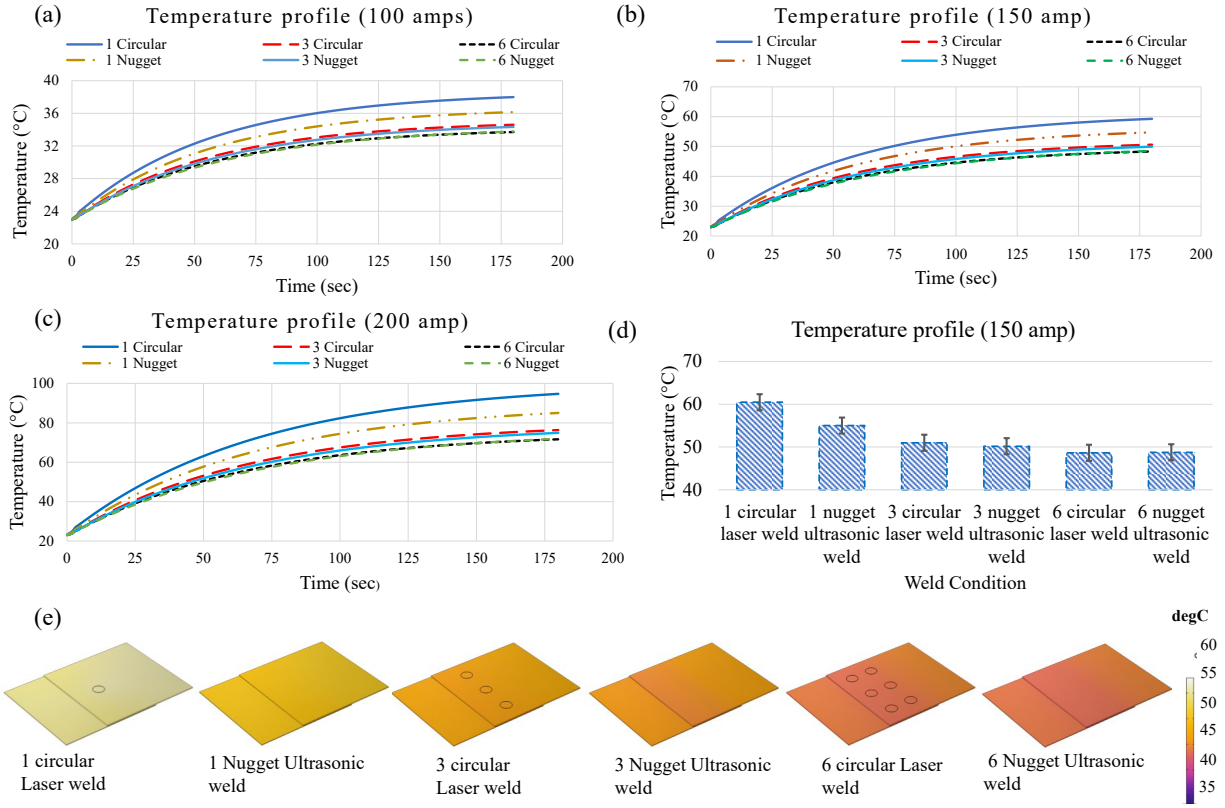

Fig. 5. Simulation-based temperature rise profile of various weld conditions (a) 100-amp, (b) 150-amp, (c) 200-amp, (d) comparison in between the weld conditions for 150 amp, and (e) simulation-based temperature maps obtained after 3 min for 150 amp.

4. Conclusion

This paper compared the impact of multiple ultrasonic weld nuggets and multiple laser-welded seams with their electrical and thermal behaviours. The drop in resistance and temperature were observed when the number of ultrasonic weld nuggets and laser welded seams were increased. A multi-physics simulation model was developed and validated with experimental results. The following conclusions can be made based on the observations:

1) The joint resistance was reduced when the number of circular laser seams or ultrasonic nuggets was increased. The laser welded seams showed comparable resistance with ultrasonic nuggets. For 3 circular laser welds showed around 2.9% less resistance than the 3-nugget ultrasonic weld.
2) The resistance and temperature analysed showed that the currently used ultrasonic joining method can be replaced with emerging laser welding and an appropriate selection of the number of joints can control the joint resistance and enhance electric vehicle safety.
3) This simulation model can be used at an early design stage to reduce joint resistance and temperature rise. This can predict the resistance and temperature profile for various weld conditions. This can be a helpful tool for battery design engineers to design a safe electric vehicle battery pack.

In conclusion, this paper demonstrated the application of the multi-physics model application for prediction and the reduction in the resistance profile of the weld joint by introducing multiple weld joints. Further work is required for details of mechanical and microstructure-based joint resistance characterisation and module scale implementation.

Acknowledgements

This research has been partially supported by a Start-up Research Grant (SRG) from the Science and Engineering Research Board (SERB), Government of India, and WMG Centre High-Value Manufacturing (HVM) Catapult, The University of Warwick, UK.

References

NITI Aayog. (2021). Handbook of Electric Vehicle Charging Infrastructure Implementation.

Das, A., Li, D., Williams, D., & Greenwood, D. (2018). Joining Technologies for Automotive Battery Systems Manufacturing. World Electric Vehicle Journal 2018, Vol. 9, Page 22, 9(2), 22.

Dimatteo, V., Ascari, A., & Fortunato, A. (2019). Continuous laser welding with spatial beam oscillation of dissimilar thin sheet materials (Al-Cu and Cu-Al): Process optimization and characterization. Journal of Manufacturing Processes, 44, 158–165.

Mohd Isa, M. S., Muhamad, M. R., Yusof, F., Yusoff, N., Brytan, Z., Suga, T., Morisada, Y., & Fujii, H. (2023). Improved mechanical and electrical properties of copper-aluminum joints with highly aligned graphene reinforcement via friction stir spot welding. Journal of Materials Research and Technology.

Mehlmann, B., Olowinsky, A., … M. T.-J. of L. M., & 2014, undefined. (2014). Spatially Modulated Laser Beam Micro Welding of CuSn6 and Nickel-plated DC04 Steel for Battery Applications. Jlps.Gr.Jp, 9(3).

Brand, M. J., Schmidt, P. A., Zaeh, M. F., & Jossen, A. (2015). Welding techniques for battery cells and resulting electrical contact resistances. Undefined, 1(1), 7–14.

Mohd Isa, M. S., Muhamad, M. R., Yusof, F., Yusoff, N., Brytan, Z., Suga, T., Morisada, Y., & Fujii, H. (2023). Improved mechanical and electrical properties of copper-aluminum joints with highly aligned graphene reinforcement via friction stir spot welding. Journal of Materials Research and Technology.

Ni, Z., Liu, Y., & Ye, F. (2022). Formation of ultrasonic spot welded Cu/Cu NPs/Cu joints and the mechanical properties and electrical resistance. Materials Science and Engineering: A, 845, 143251.

Shaikh, U. F., Das, A., Barai, A., & Masters, I. (2019). Electro-Thermo-Mechanical Behaviours of Laser Joints for Electric Vehicle Battery Interconnects. 2019 Electric Vehicles International Conference, EV 2019.

Kumar, N., Masters, I., & Das, A. (2021). In-depth evaluation of laser-welded similar and dissimilar material tab-to-busbar electrical interconnects for electric vehicle battery pack. Journal of Manufacturing Processes, 70, 78–96.

Solchenbach, T., Plapper, P., & Cai, W. (2014). Electrical performance of laser braze-welded aluminum-copper interconnects. Journal of Manufacturing Processes, 16(2), 183–189.

Wang, Q., Ping, P., Zhao, X., Chu, G., Sun, J., & Chen, C. (2012). Thermal runaway caused fire and explosion of lithium ion battery. Journal of Power Sources, 208, 210-224.

Sadeghian, A., & Iqbal, N. (2022). Blue laser welding of low thickness Ni-coated copper and mild steel for electric vehicle (EV) battery manufacturing. Optics & Laser Technology, 155, 108415.

Das, A., Masters, I., & Haney, P. (2022). Modelling the impact of laser micro-joint shape and size on resistance and temperature for Electric Vehicle battery joining application. Journal of Energy Storage, 52.

Kumar, N., Ramakrishnan, S. M., Panchapakesan, K., Subramaniam, D., Masters, I., Dowson, M., & Das, A. (2022). In-depth evaluation of micro-resistance spot welding for connecting tab to 18,650 Li-ion cells for electric vehicle battery application. International Journal of Advanced Manufacturing Technology, 121(9–10), 6581–6597.

Kumar, N., Minda Ramakrishnan, S., Panchapakesan, K., Subramaniam, D., Dowson, M., & Das, A. (2023). Utilising a novel multi-electrode approach for improving micro-resistance spot welding productivity for electric-mobility battery interconnects. Science and Technology of Welding and Joining.

Singh, A. R., Sudarsan, C., Das, A., Hazra, S., & Panda, S. K. (2022). Process Optimization and Characterization of Ultra-Thin Dissimilar Sheet Material Joints for Battery Applications Using Ultrasonic Welding. Journal of Materials Engineering and Performance, 31(5), 4133–4149.

Bandhauer, T. M., Garimella, S., & Fuller, T. F. (2011). A Critical Review of Thermal Issues in Lithium-Ion Batteries. Journal of The Electrochemical Society, 158(3), R1.

Sibilia, S., Bertocchi, F., Chiodini, S., Cristiano, F., Ferrigno, L., Giovinco, G., & Maffucci, A. (2021). Temperature-dependent electrical resistivity of macroscopic graphene nanoplatelet strips. Nanotechnology, 32(27), 275701.